Transient Thermal Analysis of Three Fast-Charging Latent Heat Storage Configurations

Therese K. Stovall*
Oak Ridge National Laboratory, Oak Ridge, Tennessee 37831
and
Rao V. Arimilli†
University of Tennessee, Knoxville, Tennessee 37996

A space-based thermal storage application must accept large quantities of heat in a short period of time at an elevated temperature. A model of a lithium hydride phase change energy storage system was used to estimate reasonable physical dimensions for this application, which included the use of a liquid metal heat transfer fluid. A finite difference computer code was developed and used to evaluate three methods of enhancing heat transfer in the phase change material energy storage system. None of the following methods, inserting thin fins, reticulated nickel, or liquid lithium, significantly improved the system performance. The use of a 95% void fraction reticulated nickel insert was found to increase the storage capacity (total energy stored) of the system slightly with only a small decrease in the system energy density (energy storage/system mass). The addition of 10% liquid lithium was found to cause minor increases in both storage density and storage capacity with the added benefit of reducing the hydrogen pressure of the lithium hydride.

Nomenclature

c_l = specific heat (liquid), J/g-K
c_p = specific heat, J/g-K
c_s = specific heat (solid), J/g-K
D = tube diameter, m
E = internal energy, J/g
Fo = Fourier number, $\alpha\tau/R_0^2$
h = heat transfer coefficient, W/m^2-K
k = thermal conductivity, W/m-K
k_l = liquid phase thermal conductivity, W/m^2-K
k_s = solid phase thermal conductivity, W/m^2-K
L = length of phase change material (PCM)
L_f = latent heat of fusion, J/g
M = number of radial divisions in finite difference grid
$\dot{m}$ = flow rate of liquid metal, g/s
N = number of axial divisions in finite difference grid
$NPIPES$ = number of PCM cylinders
Nu_x = Nusselt number, hx/k
Pe = Peclet number, VL/α
R_f = radius of liquid metal boundary, m
R_0 = radius of PCM cylinder, m
r = radial coordinate, m
Ste = Stefan number, $c_s(T_m - T_{\text{init}})/L_f$, dimensionless
s = variable of integration
T_{avg} = average of maximum inlet and outlet liquid metal temperatures, K
T_{init} = initial temperature, K
T_m = melting temperature of PCM, K
U = Kirchoff temperature, defined in Eq. 4
V = volume, m^3
$\dot{w}$ = thermal load, W
x = volume fraction of enhancement material added to PCM
z = axial coordinate, m
α = thermal diffusivity, m^2/s
ρ = density
θ = dimensionless enthalpy, defined in Eq. 10
θ^* = dimensionless cumulative energy storage, defined in Eq. 11
τ = time, s
τ_d = test duration, s
ϕ = dimensionless temperature, defined in Eq. 12

Received Sept. 12, 1988; revision received May 25, 1989; accepted for publication June 9, 1989. This paper is declared a work of the U.S. Government and is not subject to copyright protection in the United States.

*Staff Engineer.
†Professor, Mechanical and Aerospace Engineering Department. Member AIAA.

Introduction

A SPACE-BASED power system application requires a large amount of heat rejection from a power cycle in a short period of time. One proposed solution is to use a phase change thermal energy storage system to absorb the rejected heat and then release it to space over a longer period of time. The basic arrangement of the proposed storage system consists of a cylindrical tube filled with a phase change material with a high melting temperature surrounded by an annular region containing the liquid metal heat transport fluid. Lithium hydride is the preferred thermal energy storage medium because of its high latent heat and thermal conductivity and because its melting temperature matches the needs of the application.

Similar systems have been modeled in the past. However, the short time constraints for this application, coupled with the poor thermal diffusivity of the medium, lead to the consideration of three heat transfer enhancement systems: 1) the addition of thin fins, 2) the insertion of a solid lattice of reticulated nickel, and 3) the addition of a molten metal to a like metal salt (lithium and lithium hydride). In this third system, the metal is always a liquid, and the salt melts and freezes, forming a slushlike material. The reticulated nickel lattice is similar to a steel wool pad inserted into the phase change material (PCM) tube before the PCM material is poured in.

Analysis Approach

For the space-based applications under consideration, the power source may range in size from 10 to 5000 MW and may operate over a time period of 200–1500 s. For this study, a thermal storage system was sought to accept the rejected heat from a constant power source of 250 MWe (generated with a thermal efficiency of 25%) for an operational period between

900 and 1000 s. The thermal energy that must be stored is therefore approximately 7.5×10^{11} J.

The storage system is composed of a system of tubes filled with PCM that receives the rejected heat from hot liquid metal flowing on the shell side, as shown in Fig. 1. The maximum tube length permitted is about 5 m. The maximum allowable liquid metal temperature leaving the PCM storage system is 1100 K and the maximum inlet liquid metal temperature is 1200 K. The initial temperature of the PCM system is 700 K. The tube walls are made of 304SS with a tube wall thickness of about 1.27×10^{-4} m (0.005 in.).[1] An individual PCM cylinder surrounded by liquid metal modeled for this analysis is shown in Fig. 2. The PCM cylinders are radially symmetric with insulated ends. The outer boundary of the liquid metal annular volume is assumed to be adiabatic by symmetry. The liquid metal is assumed to exchange heat only within the heat exchanger and with the thermal load source. That is, outside the PCM heat exchanger, the fluid travels in an insulated pipe so that there are no upstream or downstream thermal losses. An initial temperature for the system is specified.

A heat transfer correlation based on empirical data[2-4] for a heat exchanger with NaK flowing in an annular space reported experimental results covering a range of Peclet numbers from 500 to 3000, with extrapolations down to $Pe = 40$. This correlation was chosen for use in the finite difference code because this range is appropriate for the modeled flow with a Peclet number of about 200. In Duchatelle's correlation[4] [Eq. (1)], the Nusselt and Peclet numbers are based on the hydraulic diameter $[2(R_f - R_0)]$ and the liquid metal physical properties are taken at the bulk average temperature. The value F in Eq. (1) is a factor to increase the heat transfer coefficient in the thermal and hydraulic development region. This factor was conservatively set to 1.0 for the entire tube length.

$$Nu = (6.15 + 0.02\, Pe^{0.8})F \qquad \text{for} \qquad 40 \le Pe \le 3000 \tag{1}$$

Mathematical Model

A numerical approach is used to model the behavior of a phase change storage system charged by a liquid-metal flow. A detailed discussion of the mathematical model can be found in Ref. 5. Within the PCM region, this model is very similar to that used by Solomon et al.[6] However, the geometry, element definitions, and use pattern are different. An energy balance is performed for each element in the finite difference grid. The resulting equations are solved explicitly within the PCM region and implicitly within the liquid metal region. Within the PCM region, the equations are identical to those used by Solomon et al.[6] and are based on energy conservation, Fourier's law, and the equation of state. A "Kirchoff" temperature U was defined by Solomon[6] and is useful because the position of the phase change front becomes a part of the solution rather than an assumption that must be iterated upon within the calculations. Equations (2–7) outline the energy conservation equations in terms of this Kirchoff temperature [defined in Eq. (3)].

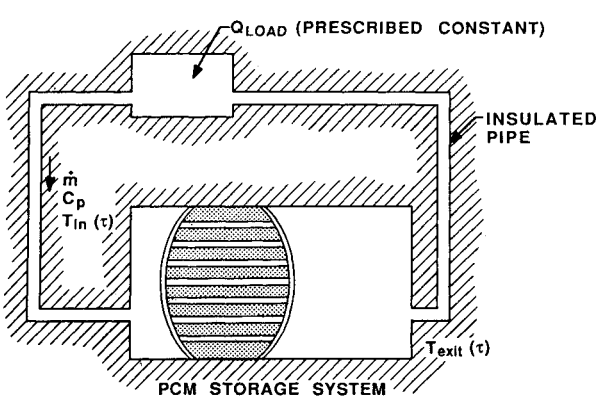

Fig. 1 System schematic.

$$K(T) = \begin{cases} k_s, & T < T_m \\ k_l, & T > T_m \end{cases} \tag{2}$$

$$U = \int_{T_m}^{T} K(s)\, ds = \begin{cases} k_s(T - T_m), & T < T_m \\ 0, & T = T_m \\ k_l(T - T_m), & T > T_m \end{cases} \tag{3}$$

$$\nabla U = K(T)\nabla T \tag{4}$$

$$\bar{q} = -\nabla U \tag{5}$$

$$\rho \frac{\partial E}{\partial \tau} = \nabla \cdot (\nabla U) \tag{6}$$

$$U = \begin{cases} \dfrac{k_s E}{c_s}, & E \le 0 \\ 0, & 0 < E < L_f \\ \dfrac{k_l (E - L_f)}{c_l}, & E \ge L_f \end{cases} \tag{7}$$

Within the liquid metal region, no phase change occurs, and hence, the Kirchoff temperature offers no advantage. The internal energy of this liquid metal region is calculated implicitly because the higher conductivity of the liquid metal requires a very small time step to avoid stability problems that occur with an explicit formulation. The code could have been improved further by recasting the entire solution as an implicit formulation.

The problem is defined in two spatial coordinates r and z and one temporal coordinate τ. Although each node represents a small, thin, cylindrical volume, the finite difference formulation is rectangular in nature. A single r-direction grid node is used for the liquid metal region because this is sufficient to determine the bulk fluid temperature as a function of z and τ. This bulk fluid temperature, in turn, is sufficient to determine the heat transfer to the PCM cylinder nodes and to test for the maximum allowable liquid metal exit temperature. After the matrix of equations is solved, the liquid metal inlet temperature is calculated using Eq. 8.

$$T^{n+1}(M + 1,1) = T(M + 1,N) + \dot{w}/\dot{m}c_p \tag{8}$$

The Kirchoff temperature approach used by Solomon is very similar to the enthalpy model discussed by Shamsundar and Sparrow.[7] Shamsundar and Sparrow used the product of Fourier and Stefan numbers (*FoSte*) as a dimensionless time parameter because it correlates the results for various values of *Ste*. The various PCM mixtures represent a range of Stefan numbers, so this product has been used in the presentation of results.

For a material with an assumed constant density and a constant latent heat, and because the internal energy variable E is defined equal to zero at the solid state melting temperature, Eq. (9) describes θ, the energy content of the PCM relative to the latent storage capacity and relative to the energy content at the solid state melting temperature. A dimensionless measure of the energy storage in the PCM can be constructed by taking the difference between the value of θ at a given point in time and the initial value of θ [see Eq. (10)]. The dimensionless temperature ϕ is defined in Eq. 11. The results are presented in terms of these dimensionless variables for generality:

$$\theta = \frac{1}{VL_f} \int_V E\, dV = \frac{1}{VL_f} \sum_{1,1}^{M,N} E_{ij} V_{ij} \tag{9}$$

$$\theta^* = \theta - \theta_{\text{init}} \tag{10}$$

$$\phi = \frac{T - T_{\text{init}}}{T_m - T_{\text{init}}} \tag{11}$$

Several factors must be considered when designing and using a finite difference computer code including time-step (in seconds) and radial and axial step (in meters) sizes. The final choice of time and element sizes (within the limits posed by model stability) is a compromise between accuracy and efficiency. The computer code running time increases at a rate roughly proportional to the number of radial divisions, from 14 Cray CPU min for $M = 3$ to 126 Cray CPU min for $M = 24$. At nine subdivisions, the predicted energy storage is within 13% and time value is within 10% of the more accurate tests. This accuracy is therefore considered acceptable considering the wide range of potential design parameters. A more complete discussion of code stability and accuracy may be found in Ref. 5. The tube wall is not modeled in the final code because the temperature gradient across the tube wall is always much smaller than the temperature difference between the liquid metal and PCM temperatures for the wall thicknesses modeled.[5]

A mixed enthalpy approach is used to model heat transfer enhancements with the finite difference code. The mixed enthalpy approach is based on an assumption that, within each computational element, the PCM mixture behaves as a homogeneous material. Knowles and Webb[8] define optimum fin dispersion requirements for which this assumption is rigorously true. They show that for cylindrical pipes absorbing heat at the walls, the fin distribution is inversely proportional to the radius. The applicability of this approach for thin fins has also been experimentally confirmed by Knowles and Webb.[8]

The mixed enthalpy method is implemented by calculating new "mixed" values for the density, heat capacity, conductivity, and latent heat of the PCM mixture [see Eqs. (12–15)]. In Eq. (13), the specific heat of each material is first converted to a volumetric specific heat (used and empirically documented by Knowles and Webb[8]), weighted according to the volumetric fraction of each material component, and finally reconverted to a mass basis using the density of the mixture. The latent heat of the mixture [Eq. (15)] must reflect not only the fact that a portion of the material does not undergo a phase change but also the new, greater density of the mixture:

$$\rho_{\text{mix}} = x\rho_{\text{add}} + (1 - x)\rho_{\text{pcm}} \tag{12}$$

$$c_{p_{\text{mix}}} = \frac{xc_{p_{\text{add}}}\rho_{\text{add}} + (1 - x)c_{p_{\text{pcm}}}\rho_{\text{pcm}}}{\rho_{\text{mix}}} \tag{13}$$

$$k_{\text{mix}} = xk_{\text{add}} + (1 - x)k_{\text{pcm}} \tag{14}$$

$$L_{f_{\text{mix}}} = \frac{\rho_{\text{pcm}}}{\rho_{\text{mix}}}(1 - x)L_{f_{\text{pcm}}} \tag{15}$$

Methods Considered for Increasing Thermal Conductivity of PCM

As will be demonstrated, the limiting factor of the PCM energy storage system is the poor conductivity of the PCM material. This conductivity is about one-tenth of the conductivity of either the liquid metal or the tube wall. If the PCM conductivity were higher, the tube radius could be larger, the number of tubes could be smaller, and the liquid metal flow rate could likely be lower.

Three enhancement methods are therefore considered in this study. They involve replacing some portion, measured as a volume percent, of the PCM with 1) a reticulated metal insert, 2) thin fins, or 3) liquid lithium (to make a metal salt/molten metal slurry). Both aluminum and nickel are available as a reticulated material (similar to steel wool) with void fractions from 90 to 95%. Aluminum has a much higher conductivity but unfortunately a melting point below the application under consideration. Nickel is therefore chosen as the material for the reticulated metal insert. Both 90 and 95% void fractions are modeled. The fins are made out of the same material as the tube wall, 304SS. Fin volume fractions from 5 to 50% are modeled. The metal/metal-salt mixture is generated by adding liquid lithium to the lithium hydride salt. This addition not only improves the heat transfer but is also valuable because it significantly reduces the PCM's hydrogen pressure due to dissociation of the hydride. This reduction, in turn, simplifies the PCM containment problem. Volume fractions of the liquid lithium from 10 to 50% are modeled.

Results

The configuration chosen as a basis for comparison to the enhanced systems is shown in Table 1 under the heading "Base configuration." It has $R_0 = 0.05$, $L/D = 5$, and $NPIPES = 4000$. The high (about 60%) proportion of sensible heat storage in the PCM is largely attributable to the difference between the initial system temperature of 700 K and the PCM melt temperature of 962 K.

The amount of energy stored in the liquid metal heat transfer fluid was about 1.5 times the amount of energy stored in the PCM tube. Because of this ineffective distribution of energy storage, several other configurations were tested, with smaller radii and with smaller R_f/R_0 ratios. Most of these cases were unable to satisfy the operating period requirements. However, one test case (also shown in Table 1) did satisfy this requirement and shows that the system base configuration chosen is far from optimum. Based on this example, and on the large number of system parameters that could be varied, the system performance reported in this study should be used only to measure the relative value of system modifications, not as an absolute measure of potential system performance.

The reticulated nickel, liquid lithium, and steel fins have a modest effect on system performance, increasing both the length of time for which the thermal load could be met and the total energy stored. The decrease in energy storage density (energy stored/system mass) varies greatly among these three modifications. The following comparisons are based on a maximum operating period of 1000 s, as described in the problem definition. Some alternative bases for comparison are also discussed.

The operational period of the base system is 947 s. The addition of thin fins and the insertion of reticulated nickel material increases the operational period beyond 1000 s. The addition of liquid lithium increases the operational period to 960 s for a 10% addition; however, the operational time for larger additions is decreased.

The amount of energy stored is increased by up to 6% by the use of a reticulated nickel insert or by the addition of thin fins, as seen in Fig. 3. The energy storage benefits of the 90 and 95% void fraction nickel inserts are the same. Two-thirds of the energy storage increase attainable by the addition of thin fins is available at only a 10% volume addition. The energy storage does not increase at all when the volume fraction of the fin material is increased further from 30 to 50%.

Table 1 System configurations[a] based on finite difference analysis

System parameter	Base configuration	Improved configuration
R_f/R_0	3	2.0
R_0	0.05	0.03
L/D	50	83
Number of PCM tubes	4,000	19,000
Ratio of latent to sensible storage in PCM	0.434	0.504
θ^*	1.11	1.246
Ratio of energy stored in liquid metal to energy stored in PCM	1.6	0.41
System[b] energy density, J/g	691	973

[a]Liquid metal velocity = 0.04 m/s, $R_f/R_0 = 3$.
[b]System includes tube wall and liquid metal in annular region.

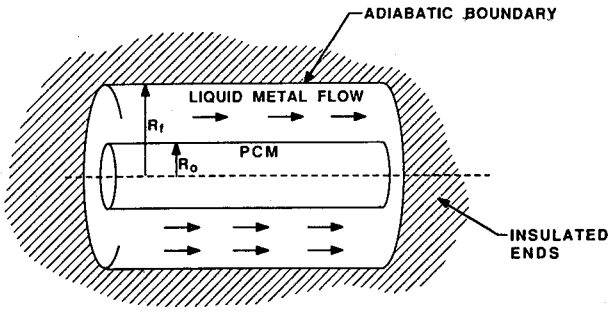

Fig. 2 Model schematic.

The addition of liquid lithium increases the energy storage a small amount for additions of 10% or less. Larger amounts of liquid lithium actually decrease the energy storage capacity. This decrease is attributable to the low density of liquid lithium, lower even than the PCM. Since the volume of each tube is held constant, increasing the proportion of liquid lithium decreases the mass of the PCM mixture. The opposite is true for both reticulated nickel and fin configurations.

For the specified operating period range, the energy storage density is decreased by the use of fins and the reticulated nickel insert but is relatively unchanged by the addition of liquid lithium (see Fig. 4). The thin fin and nickel additions of 10% decrease the energy storage density by about 7%.

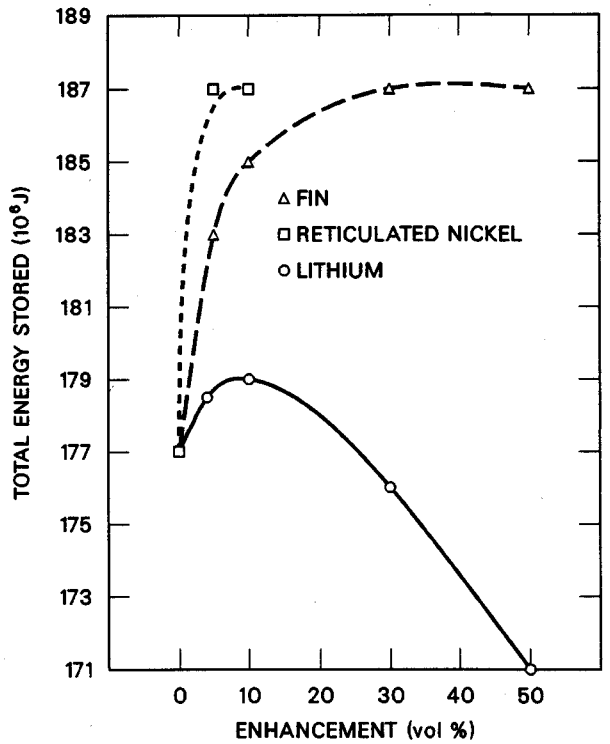

Fig. 3 Effect of enhancements on total energy storage.

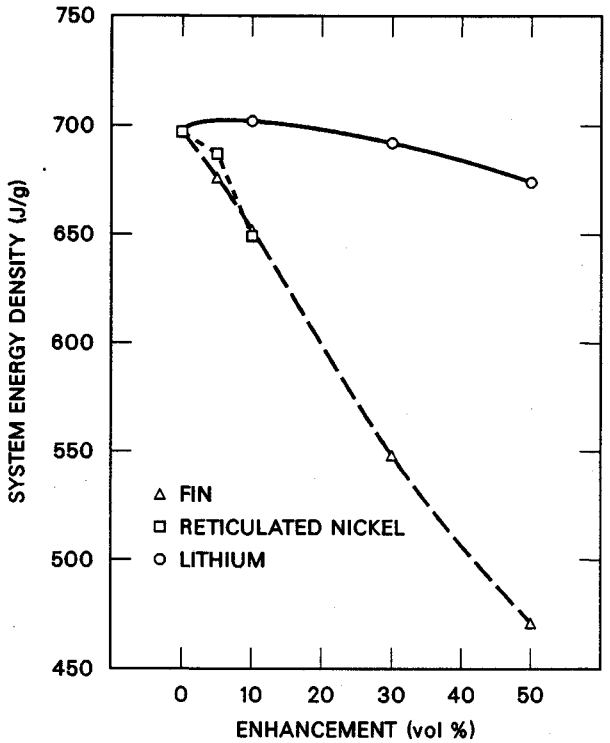

Fig. 4 Effect of enhancements on system energy density.

Table 2 Performance summary of enhanced systems[a]

Enhancement, volume %	Thermal diffusivity, 10^{-6} m²/s	*FoSte*[b]	Test[b] duration	System[c] energy density, J/g	PCM[d] energy stored, 10^6 J/tube	θ^*	Total energy[e] stored, 10^6 J/tube	Ratio of latent to sensible energy storage in the PCM	Ratio of energy stored in liquid metal to energy stored in PCM
				Reference case, no enhancement					
0	0.9	0.27	947	697	66.0	1.11	177	0.43	1.6
				Reticulated nickel					
5	1.5	0.47	1000	687	76.7	1.35	187	0.53	1.4
10	2.0	0.69	1000	649	77.1	1.48	187	0.56	1.3
				Liquid lithium					
10	1.2	0.36	960	702	71.0	1.27	179	0.47	1.6
30	1.7	0.59	942	692	73.0	1.58	176	0.50	1.6
50	2.4	1.00	914	674	73.1	2.03	171	0.50	1.8
				304 SS thin fins					
5	1.1	0.36	978	676	72.4	1.26	183	0.47	1.5
10	1.4	0.46	992	652	75.8	1.38	185	0.50	1.4
30	2.3	0.97	1000	548	79.6	1.85	187	0.53	1.4
50	3.4	1.91	1000	471	81.7	2.52	187	0.48	1.4

[a] $R_0 = 0.05$ m, $R_f/R_0 = 3$, $v = 0.04$ m/s, $L/D = 50$, *NPIPES* = 4000.
[b] Computer model stops when liquid metal exit temperature reaches 1100 K or at 1000 s, whichever comes first.
[c] System includes liquid metal region and tube wall.
[d] Includes only enhanced PCM material.
[e] Includes energy stored in the form of increased internal energy of liquid metal in the annular region.

Figure 5 shows that a reticulated nickel insert with a 95% void fraction offers the best compromise between an increase in storage capacity and a relatively small decrease (~1%) in the energy storage density for the specified operating period range. An addition of 10% liquid lithium increases both the energy storage density and the total energy storage capacity, but only by a very small amount. However, this option has the added benefit of reducing the hydrogen pressure of the lithium hydride PCM.

The ratio of energy stored in the form of latent heat to the sensible heat within the PCM varies from 0.43 in the base configuration to 0.56 in the 90% void fraction reticulated nickel insert configuration, as Table 2 shows. If all the PCM in the base configuration (starting from an initial temperature of 700 K) were melted and at the melting temperature, this ratio would equal a value of 1.3. However, much of the PCM remains unmelted at the end of the operating period. Also, the PCM nearest the surface heats up above the melting temperature, further increasing the proportion of sensible heat storage.

The position of the phase change front at the end of the operating period is calculated. The front for most of the cases only penetrates about 25% of the way into the PCM. However, at an r/R_0 value of 0.75, about 44% of the PCM volume is in the melted zone. The center of the PCM is melted only for very large additions of liquid lithium or fins. Such large additions are not supported by the energy storage and energy density considerations already discussed.

It is interesting to note, however, that doubling the volume percent of reticulated nickel or thin fins from 5 to 10% has a relatively small effect on the interface location, as does tripling the liquid lithium from 10 to 30%. However, tripling the fin volume from 10 to 30% has a very large effect, moving the interface all the way to the center of the PCM tube for $z/L < 0.2$. Increasing the fin volume by another 67% (from 30 to 50% volume) causes the melting front to reach the center for 80% of the length of the tube. Also, increasing the liquid lithium fraction from 30 to 50% (only a 67% increase) causes a tremendous increase in melt front propagation for $z/L < 0.1$.

Figure 6 shows the dimensionless temperature response of the central ($r = 0$, $z/L = 0.5$) PCM node vs the dimensionless time variable that reflects the varying Stefan numbers of the modified PCM. The nondimensional temperature response is slightly slowed by additional amounts of enhancement material (i.e., $\partial\phi/\partial FoSte$ is decreased as the thermal diffusivity is increased). The nondimensional behavior reflects the fact that the *FoSte* time parameter is proportional to the increasing thermal conductivity of the enhanced materials. This increasing thermal conductivity stretches the time scale, causing this counter-intuitive trend. However, for the real-time data shown in Fig. 7, the time response is improved (i.e., $\partial T/\partial\tau$ is increased) by the addition of the enhancement materials.

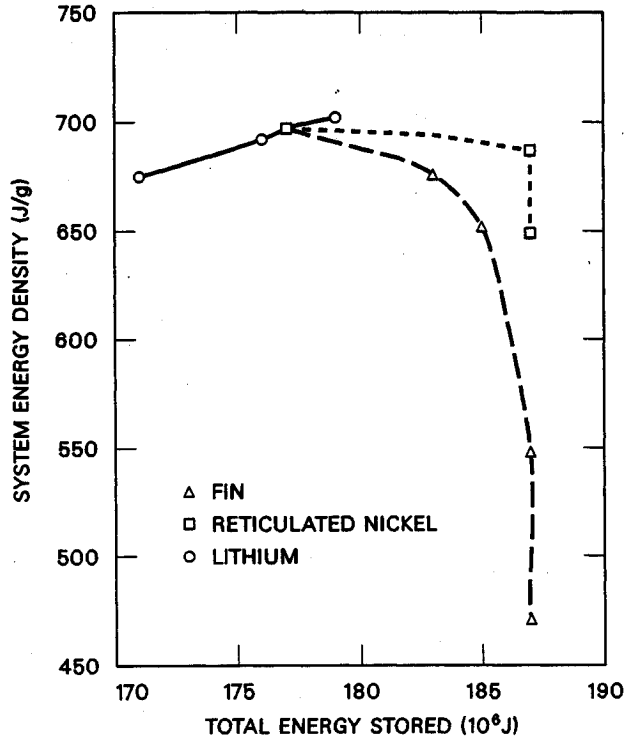

Fig. 5 System energy density vs total energy stored for enhanced systems.

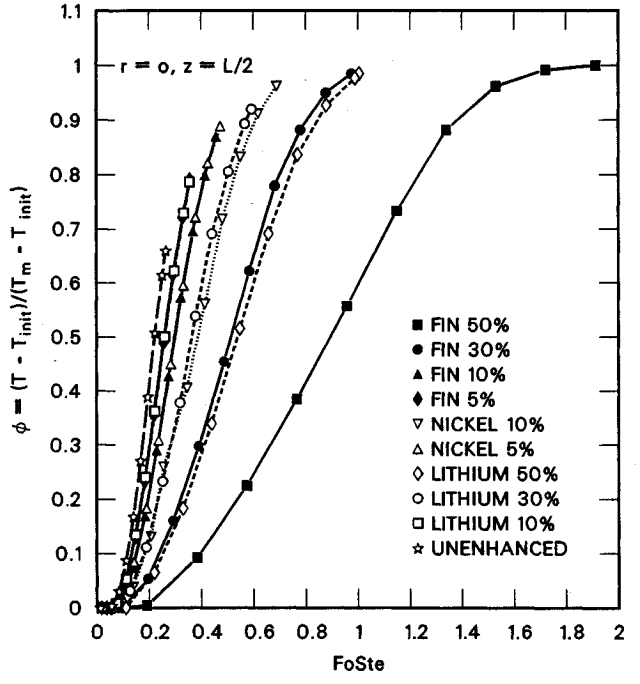

Fig. 6 Nondimensional time response of central PCM node for enhanced configurations.

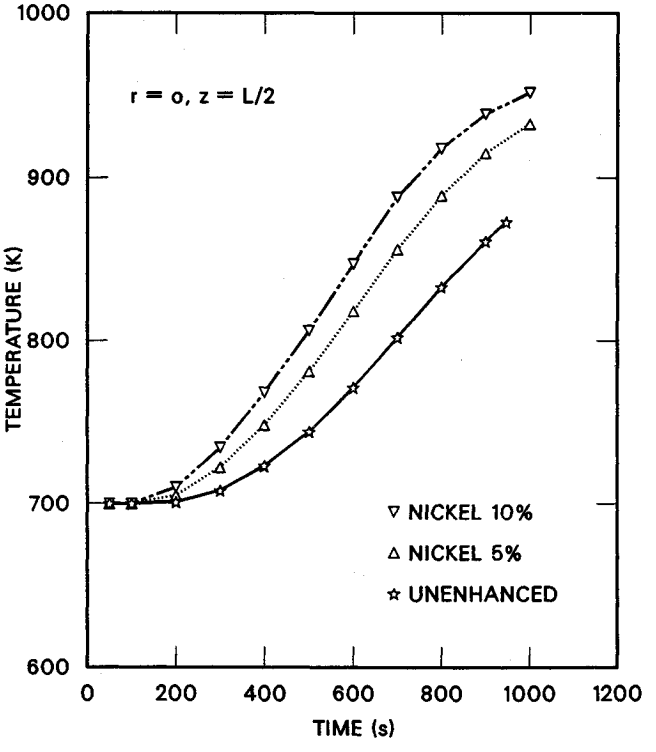

Fig. 7 Temperature response of central PCM node for systems enhanced with reticulated nickel.

The performance comparisons discussed so far were based on a strict adherence to the problem definition. Specifically, operating periods longer than 1000 s were not considered even though some of the modified systems were capable of receiving and storing more thermal energy without exceeding the liquid metal inlet and outlet temperature constraints. If the application of this thermal storage system was well defined and unlikely to change, this basis for comparison would be unquestioned. However, given the latitude in current applications requirements, further discussion of the performance of these systems is in order.

If the comparison were based solely on the system's physical dimensions and on the inlet and outlet liquid metal temperature constraints, several conclusions reached using the 1000-s limit would be different. For the reticulated nickel insert, the most important change is that now the total energy stored for the reticulated nickel insert continues to increase from 187 MJ to 197 MJ as the volume percent of nickel is increased from 5 to 10%. As the void fraction drops from 95 to 90%, the system energy density is decreased by only 20 J/g rather than the sharper drop of almost 40 J/g with the 1000-s limit. This would change the conclusion that the 95% void fraction material is clearly more effective than the 90% void fraction material. The choice between these two void fractions then should be based on a more subtle trade-off among increased storage capacity, lengthened operating period, and slightly decreased system energy density.

The effect of this approach on the fin results is not as dramatic because the overall system energy density is still decreased substantially by the use of such fins. However, it becomes apparent that a maximum energy storage capacity occurs somewhere between 10 and 50% fin volume. The operating period is also slightly longer within this range.

Considering the changeable nature of these conclusions, some word of caution should accompany the results of this study. It would appear that the most appropriate system comparison should be based on optimized parameters for each enhanced system. However, such an optimization strategy was beyond the scope of this study. The development of such a strategy should be pursued if this type of thermal storage system remains a viable candidate in the overall system design.

Summary

A PCM energy storage system application included a short charging period and the use of a liquid metal heat transfer fluid. A finite difference computer code was developed and used to evaluate the effect of three heat transfer enhancements on the PCM energy storage system.

For a maximum operating period of 1000 s, the use of a 95% void fraction reticulated nickel insert was found to increase the storage capacity of the system by ~6% with a decrease in the system energy density of only ~1%. For the given physical system, the storage capacity can be increased still further if the operating period is not constrained. The addition of 10% liquid lithium was found to cause minor increases in both storage density and storage capacity with the added benefit of reducing the hydrogen pressure of the lithium hydride PCM.

The base system used for comparison with the various modifications was not an optimized configuration. Based on a limited examination of other potential system configurations, significant performance improvements are possible. Such an optimization effort should be pursued if these configurations continue to be considered as candidate solutions. Any computer model used for this optimization should be based on a fully implicit solution approach, an improvement over the partially implicit solution used for this study. It also appears that a small addition of the liquid lithium might be considered in conjunction with the reticulated nickel, thereby gaining both the increased storage capacity and the reduced hydrogen pressure benefits of these two enhancements.

Acknowledgment

This research was conducted at the Oak Ridge National Laboratory, Oak Ridge, Tennessee, operated by Martin Marietta Energy Systems, Inc. for the U.S. Department of Energy under Contract DE-AC05-840R21400.

References

[1]Foote, J. P., Morris, D. G., and Olszewski, M., "Encapsulated Sink-Side Thermal Energy Storage for Pulsed Space Power Systems," 22nd Intersociety Energy Conversion Engineering Conf., Philadelphia, PA, Aug. 1987.

[2]Duchatelle, L., de Nucheze, L., and Robin, M. G., *Future Energy Production Systems: Heat Transfer in Helical Tube Sodium Heated Steam Generators,* Vol. 1, edited by J. C. Denton and N. H. Afgan, Academic Press, New York, 1976.

[3]Valette, M., "A Heat Transfer Study for Vertical Straight-Tube Steam Generators Heated by Liquid Metal," *Liquid Metal Engineering and Technology,* Vol. 2, Proceedings of the Third International Conf., Oxford, England, UK, April 1984, British Nuclear Energy Society, London, 1984.

[4]Duchatelle, L., and de Nucheze, L., "Determination des Coefficients de Convection d'un Alliage Sodium-Potassium Circulant a Contrecourant dans un Echangeur Monotubulaire," *Entropie,* No. 17, Sept.-Oct. 1967, pp. 51-58.

[5]Stovall, T. K., "Transient Thermal Analysis of Three Latent Heat Storage Configurations for Rapid Thermal Charging," Oak Ridge National Lab., ORNL/TM-10719, Oak Ridge, TN, June 1988.

[6]Solomon, A. D., Morris, M. D., Martin, J., and Olszewski, M., *The Development of a Simulation Code for a Latent Heat Thermal Energy Storage System in a Space Station,* Oak Ridge National Lab., ORNL-6213, Oak Ridge, TN, April 1986.

[7]Shamsundar, N., and Sparrow, E. M., "Analysis of Multidimensional Conduction Phase Change Via the Enthalpy Model," *Journal of Heat Transfer,* Vol. 97, Aug. 1975, pp. 333-340.

[8]Knowles, T. R., and Webb, G. W., *Metal/Phase-Change Material Composite Heatsinks,* Energy Science Lab. for Flight Dynamics Lab., AFWAL-TR-88-3069, Wright-Patterson AFB, OH, 1988.